Fibers and Polymers 2015, Vol.16, No.1, 95-104
DOI 10.1007/s12221-015-0095-9

ISSN 1229-9197 (print version)
ISSN 1875-0052 (electronic version)

Thermoplastic Polyurethane/Polypropylene Blends in a Co-rotating Non-twin Screws Extruder

Jia-sheng Luo[1,2], Bai-ping Xu[1,2]*, Hui-wen Yu[1], Yao-xue Du[2], and Yan-hong Feng[3]

[1]*Technology Development Center for Polymer Processing Engineering of Guangdong Colleges and Universities, Guangdong Industry Technical College, Guangzhou 510300, China*
[2]*College of Mechanical and Electrical Engineering, Wuyi University, Jiangmen Guangdong 529020, China*
[3]*National Engineering Research Center of Novel Equipment for Polymer Processing, South China University of Technology, Guangzhou 510640, China*

(Received May 16, 2014; Revised July 14, 2014; Accepted July 27, 2014)

Abstract: Thermoplastic polyurethane (TPU)/polypropylene (PP) blends of different weight ratios were prepared with a self-made co-rotating non-twin screws extruder (NTSE), which rotates at a speed ratio of 2.0, and a traditional twin-screw extruder (TSE), which rotates at a speed ratio of 1.0. The mechanical properties, phase morphology and thermal stabilities were investigated to characterize the effect of different processing methods. The experimental results revealed that the samples prepared with a NTSE had superior mechanical properties compared to those of the samples prepared with a TSE. High-resolution scanning electron microscopy showed a structure feature of fiber morphology of TPU/PP blends prepared with a NTSE and the particle size of dispersed phase of blends prepared with NTSE is smaller than that prepared with TSE, indicating that the NTSE is more efficient in mixing for immiscible polymer blends. Furthermore, thermogravimetric analysis curves indicated the strong interaction of the TPU/PP blends influenced by the flow field in NTSE, compared to that of TSE-extruded.

Keywords: Non-twin screws, Extrusion, Mixing, Morphology, Mechanical properties

Introduction

Polypropylene (PP), a semi-crystalline polyolefin plastomer, is an outstanding polymer material with respect to its wide property spectrum performance, in particular, its ease of processing, good chemical resistance, rigidity and heat resistance, and relatively low cost [1], however, the large shrinkage ratio, low temperature brittleness and low abrasion performance limit its application. TPU is the system with microphase-separated domains composed of relatively flexible soft segments and stiff hard segments. Incorporating TPU into PP can improve the impact toughness of PP at low temperature. The TPU/PP blend with ethylene-vinyl acetate is homogeneous with higher mechanical strength than that of the commercial PVC blood bag [2]. Actually, TPU and PP blends are highly immiscible because of the large differences in their polarities and their high interfacial tensions [3]. Previous studies on the binary blends included the work by Macosko who studied the compatibility of PP-g-MA, PP-g-NH_2 and PP-g-NHR with TPU for different compositions [4]. The result showed that compatibility of PP-g-NHR with TPU was the best. Potschke [5,6] studied the morphology and properties of thermoplastic polyurethanes/polyolefines blends with different viscosity ratios and found that the higher viscosity ratios of TPU/PE blends show a lower dispersity than TPU/PP blends. To improve the mechanical properties of the TPU/PP blends, Kannan *et al.* [7]. produced the TPU/PP nanocomposites with clay by melt mixing using a twin-screw extruder. They found that the clay could reduce the surface energy of the TPU hard segments and make them more compatible with the nonpolar PP. Moreover, Petra Potschke and Katrin Wallheinke [8] investigated the morphology and mechanical properties of TPU/PE-g-MA blends in a twin-screw extruder. With PE-g-MA as blend component, the particle size was dramatically reduced in comparison with PE and the phase adhesion and the mechanical properties were all improved.

The aforementioned work was commonly carried out in a traditional twin-screw extruder (TSE) or batch mixer governed by conventional shear flow. Qu [9] improved the shear flow by the introduction of the vibrational force field and studied the relationship between the crystallization behavior of isotactic polypropylene (iPP) and the vibration shear conditions. The result showed that with the increase of the vibration amplitude, the melt point of iPP and the degree of crystallinity increased. In addition, several studies have reported that the melted drops in polymer processing were more efficiently broken under elongational flow [10-14]. Some researchers [15,16] attempted to generate elongational flow with fixed equipment. Qu [17] invented a novel plasticizing apparatus known as the van extruder to generate the higher stress and the dynamical elongational flow. Xu [18] attempted to introduce the asymmetrical effect into the screw channel to enhance the chaotic mixing and elongational flow. It follows that a novel co-rotating non-twin screws extruder (NTSE) was invented. The further 2D numerical simulation showed that the distributive mixing and dispersive mixing in NTSE were superior to those in TSE [19].

*Corresponding author: xubaiping2003@163.com

In the present work, we compared the reinforcement mechanical properties and enhancement mixing performance for TPU/PP blends of various weight ratios on the basis of novel NTSE and conventional TSE. Mechanical properties, morphological properties and thermal stabilities of the blends were examined. Emphasis is placed on the effect of the flow field on the mixing performance and interaction of the TPU/PP blends in a NTSE.

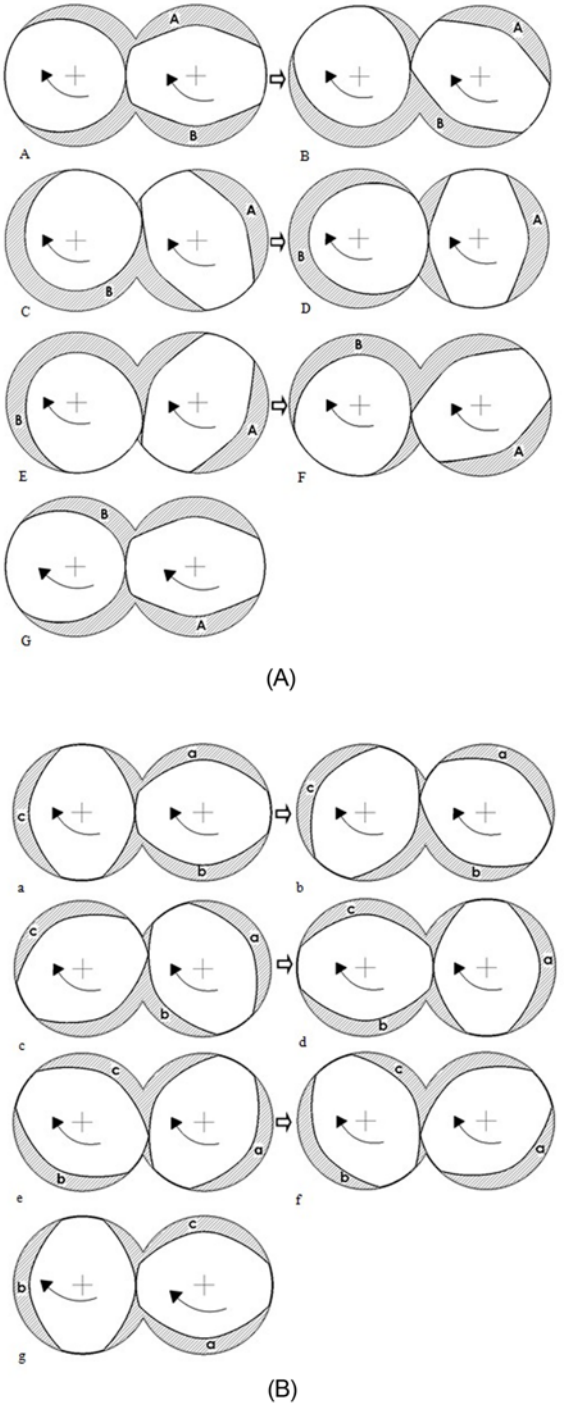

Figure 1. The cross sections for screws in corotating kneading disk pairs; (A) NTSE and (B) TSE.

Experimental

Extrusion Device

The geometry of fully wiped twin-screw equipment has been discussed by Booy [20]. The traditional co-rotating twin screws commonly used in industry application have identical cross sections arranged at the certain phase angle and rotate at the same speed. The NTSE invented by Xu consists of two screws with the same diameter and a speed ratio of 2.0. The cross sections for screws in corotating kneading disk pairs are shown in Figure 1. Further, the 3D views for screw element and motion paths of materials are shown in Figure 2. Materials have more chance to be exposed to the nip regions in NTSE to accelerate the melting, compared to those in TSE.

Figure 3 depicts the screw configurations in NTSE and TSE. Here 48/96 represents a screw element with a pitch of 48 mm and an axial length of 96 mm while 45 °/5/20 stands for a kneading disk with 5 kneading paddles (each at a staggered angle of 45 °) and an axial length of 20 mm. The

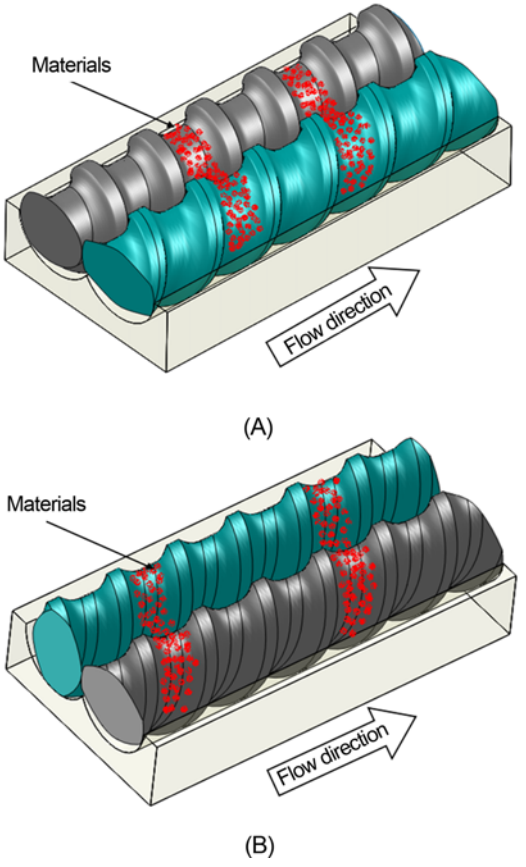

Figure 2. 3D views for screw element; (A) NTSE and (B) TSE.

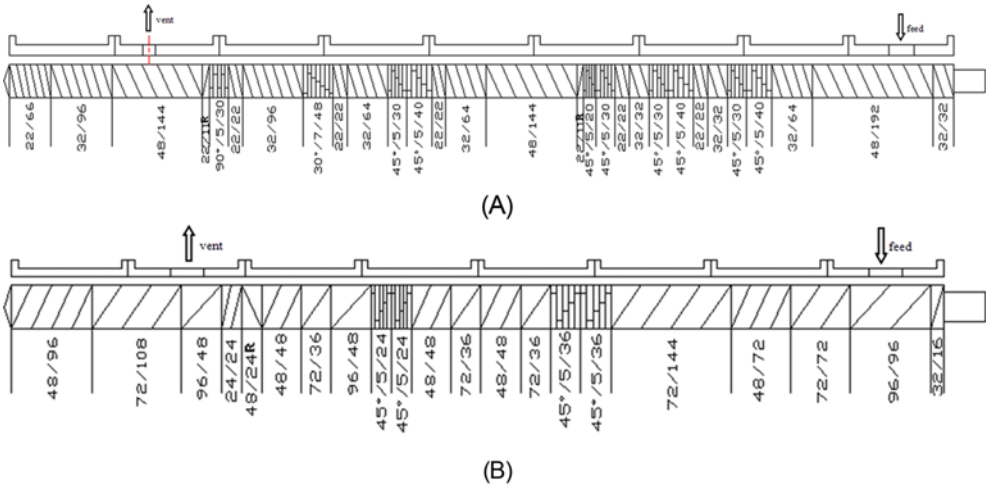

Figure 3. Arrangement of screw elements for different co-rotating extruders; (A) screw configuration in TSE and (B) screw with two tips configuration in NTSE.

co-rotating twin-screw extruders are flexible devices because of their modular structure. The diameters of the screws are 35 mm, and their centerline distance is 30 mm. The length/diameter (L/D) was 42.7 in TSE and 32 in NTSE, respectively. Remarkably, TSE consists of ten groups kneading disks and two reverse screw elements as shown in Figure 3(A), in contrast, there are only four groups kneading disks and one reverse screw element in NTSE as shown in Figure 3(B). Obviously, fewer kneading disks will result in less damage on matrices of composite because of the less shear action.

Materials and Preparation

PP (grade T30S, isotaxy type) was obtained from China Petroleum and Chemical, and the melt flow index and density provided by the supplier were 3.0 g/10 min and 0.91 g/cm^3, respectively. TPU (grade 1190A, polyester type) was supplied by the chemical company of BASF, and the shore A hardness and density provided by the supplier were 92 and 1.14 g/cm^3, respectively. All of the materials were dried in an oven at 80 ^{o}C for 2 h before processing. Maintaining the feed rate and screw with two tips speed constant in NTSE and TSE, the TPU/PP blends with different weight ratios of 10/90 to 90/10 were directly extruded through the die with 3 mm holes and the samples were obtained after cooling. The samples with TPU/PP weight ratios of 10/90 to 90/10 were used to study the interface morphology. The blends with the TPU/PP weight ratios of 10/90, 50/50, 70/30 and 90/10 were used to investigate thermal stabilities.

Table 1 presents the processing conditions of blends in the experiment. The specimens used for the measurement of mechanical properties were compression-molded in a hydraulic press at 200 ^{o}C. The blend with 10 % TPU was molded in a injection machine. The specimens used to measure the phase morphology, thermal behavior, and mechanical properties were put in a room at 25 ^{o}C for 24 h before measuring.

Mechanical Testing

CMT4204 electronic universal testing machine was used, which was produced by MTS systems (China) Co., Ltd. The tensile speed was kept at 20 mm/min. For testing the tensile modulus, the tensile speed was 1 mm/min. GB/T 1040.2-2006 standard was used in the test. The dimensions of the testing specimens were carefully machined to be 75×5×2.5 mm by dumbbell mold. All the tests were performed at the temperature of 25 ^{o}C. Five specimens were used in each test to obtain the average value.

Scanning Electron Microscopy (SEM)

A field emission scanning electron microscope (JSM-6330F) was used to study the morphology, which was produced by Japan Electron Optics Laboratory Co., Ltd.. The samples were fractured in liquid nitrogen and covered with gold before being examined with the microscope.

Thermogravimetric Analysis (TGA)

TG measurements were performed using a DSC/TGA

Table 1. Processing conditions of blends

Extruder	Screw speed (rpm)	Processing temperature (^{o}C)	L/D	Output
NTSE	24	170-185-190-195-200-200-200-200-195	32	3.32 kg/h
TSE	24	160-170-180-185-190-195-200-200-200-195	42.7	3.48 kg/h

synchronous testing machine under a nitrogen atmosphere in order to study the thermal stabilities of TPU/PP blends. Specimens of approximately 7 mg were heated from 30 to 600 °C at the heating rate of 10 °C/min. From the TG curves, thermal degradation features such as the beginning degradation temperature (T1), the terminal degradation temperature (T3), the maximum rate of degradation temperature and the temperature at different mass losses were presented.

Results and Discussion

Mechanical Properties

Figure 4 illustrates the mechanical properties (i.e., tensile strength, elongation at break, tensile modulus, and impact strength) of the TPU/PP blends with various TPU contents extruded by NTSE and TSE. The V-shaped tensile strength curves of TPU/PP blends were found with increasing TPU weight content for both cases. As shown in Figure 4(A), the decrease in the tensile strength reveals that the blends had weak interface interaction. Incorporated PP may cause disruption in the TPU interchange of hydrogen bonding, facilitate crack propagation at weak phase interfaces, and thereby lower the tensile strength of the blends [21]. The tensile strength of NTSE-extruded specimens with high TPU content (>50 %) was higher than TSE-extruded blends and the lowest value was found when TPU proportion was about 60 %. The minimum of 60 % content acts like a breaking point in the strength versus composition curve, which indicates a substantial structural and morphological change caused by phase inversion [22]. Thus, TPU make up continuous phase with PP as dispersive phase when TPU proportion was above 60 %. Figure 4B demonstrates the elongation at the break of blends of various PP contents. With increasing TPU weight content, the approximate flat zone emerged, which covered the TPU content from 20 % to 50 %, after a slight decrease from 10 % TPU content to 20 %, and the elongation showed an increasing trend. Because of the high immiscibility of TPU/PP blends, the crack at weak phase interfaces increase with the increasing TPU weight ratio. Anyway, the elongations of the blends extruded by NTSE were larger than those of the samples prepared with a TSE. Figure 4(C) depicts the tensile modulus of the TPU/PP blends of various TPU components. The tensile modulus reduced with increasing TPU weight

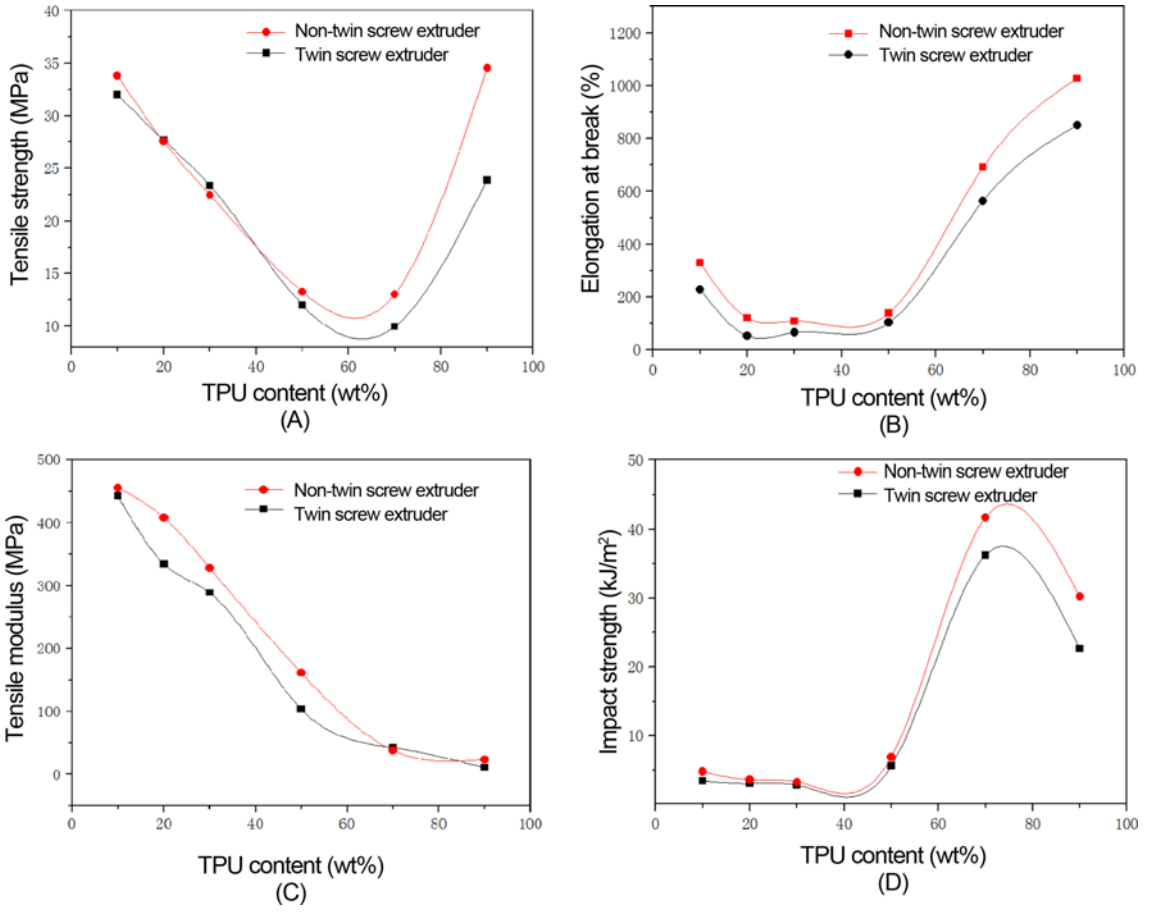

Figure 4. Mechanical properties as functions of blend composition; (A) tensile strength, (B) elongation at break, (C) tensile modulus, and (D) impact strength.

content. The tensile modulus of TPU/PP (10/90) blend prepared with a NTSE was about twenty times than that of TPU/PP (90/10) blend. The great reduction of tensile modulus in the blends indicates that the TPU/PP blends become more soft and prone to elastic deformation. Figure 4(D) illustrates the impact strength of the TPU/PP blends with various TPU contents. The impact strength of the blends with high TPU content significantly improved. The impact strength increased remarkably especially for sample with 90 % TPU content, indicating that a strong interface could effectively transfer stress [23]. Further, the mechanical properties of the TPU/PP blends prepared with NTSE were superior to those of the samples prepared with TSE, as shown in Figure 4.

Figure 5 illustrates the stress-strain curves of TPU/PP blends with various TPU contents. For the case of the blend with 10 % TPU weight ratio, the tensile strength of the blend extruded by NTSE was 28.09 MPa in contrast to 26.52 MPa of TSE-extruded blend. For the case of the blend with 50 % TPU weight ratio, it was 11.25 MPa in contrast to 9.47 MPa, and for the case of the blend with 90 % TPU weight ratio, it was 5.73 MPa in contrast to 5.21 MPa. These results indicate that the tensile strength decreased with the increase of TPU content. Similarly, the tensile strength and tensile modulus of specimens prepared with NTSE were all greater than those of the samples prepared with TSE.

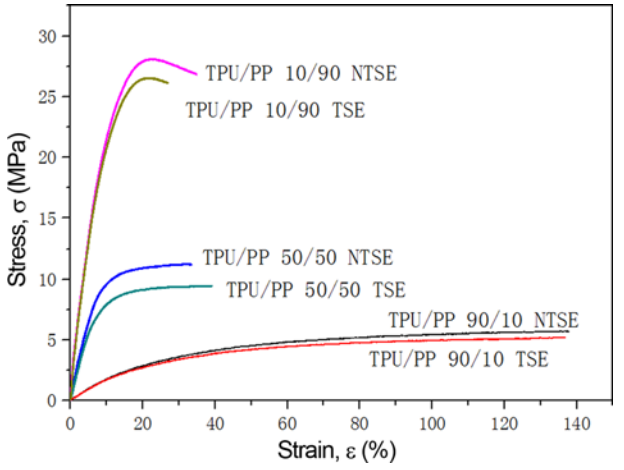

Figure 5. Stress-strain curves of TPU/PP blends extruded by NTSE and TSE.

Table 2 presents the mechanical properties of TPU/PP blends extruded by NTSE and TSE with different TPU components. The mechanical properties of the blend with 90 % TPU content extruded by NTSE were greatly improved compared to other blends with different TPU components.

Table 3 depicts the comparison of mechanical properties of TPU/PP (10/90) blend with different molding methods. The specimens were molded either by injection molding or by compression molding. The mechanical properties of NTSE-extruded blend were superior to those of TSE-extruded blend. However, because the blend experienced shear flow mixing in the injection molding once more, the mechanical properties of injection molded blend were greater than those of compression molded blend.

Morphology Analysis

High-resolution SEM observations are performed to examine the differences in dispersion particle morphology in the TPU/PP blends extruded by novel NTSE and conventional TSE. Figures 6 and 7 show the dispersion-phase morphology of the TPU/PP blends from fresh extruder dies of NTSE and TSE. The dispersive phase underwent the phase reversion when the TPU content was above 60 %. It was found that the particle size of dispersed phase of blends prepared with NTSE is smaller than that prepared with TSE. In addition, when the TPU was in the dispersed phase, the particle size was small at low TPU content (⩽20 %). The particle size

Table 3. Comparison of mechanical properties with different molding method (10 %TPU)

Molded method	Extruder	Tensile strength (MPa)	Impact strength (kJ/m^2)
Injection	NTSE	36.86	5.44
	TSE	34.67	5.20
Compression	NTSE	33.80	4.78
	TSE	32.02	3.43

Table 2. Mechanical properties of TPU/PP blends extruded by NTSE and TSE

Blend content (TPU/PP)	Extruder	10/90	20/80	30/70	50/50	70/30	90/10
Tensile strength (MPa)	NTSE	33.80	27.55	22.46	13.25	13.02	34.58
	TSE	32.02	27.66	23.37	12.00	9.94	23.89
Elongation at break (%)	NTSE	329.47	120.43	108.85	139.65	691.7	1028.18
	TSE	228.60	52.45	66.23	102.87	563.5	850.6
Tensile modulus (MPa)	NTSE	455.72	408.21	328.19	161.03	37.67	23.43
	TSE	443.26	334.54	288.72	103.25	42.2	10.54
Impact strength (kJ/m^2)	NTSE	4.78	3.59	3.28	6.90	41.72	30.21
	TSE	3.43	3.06	2.81	5.63	36.25	22.66

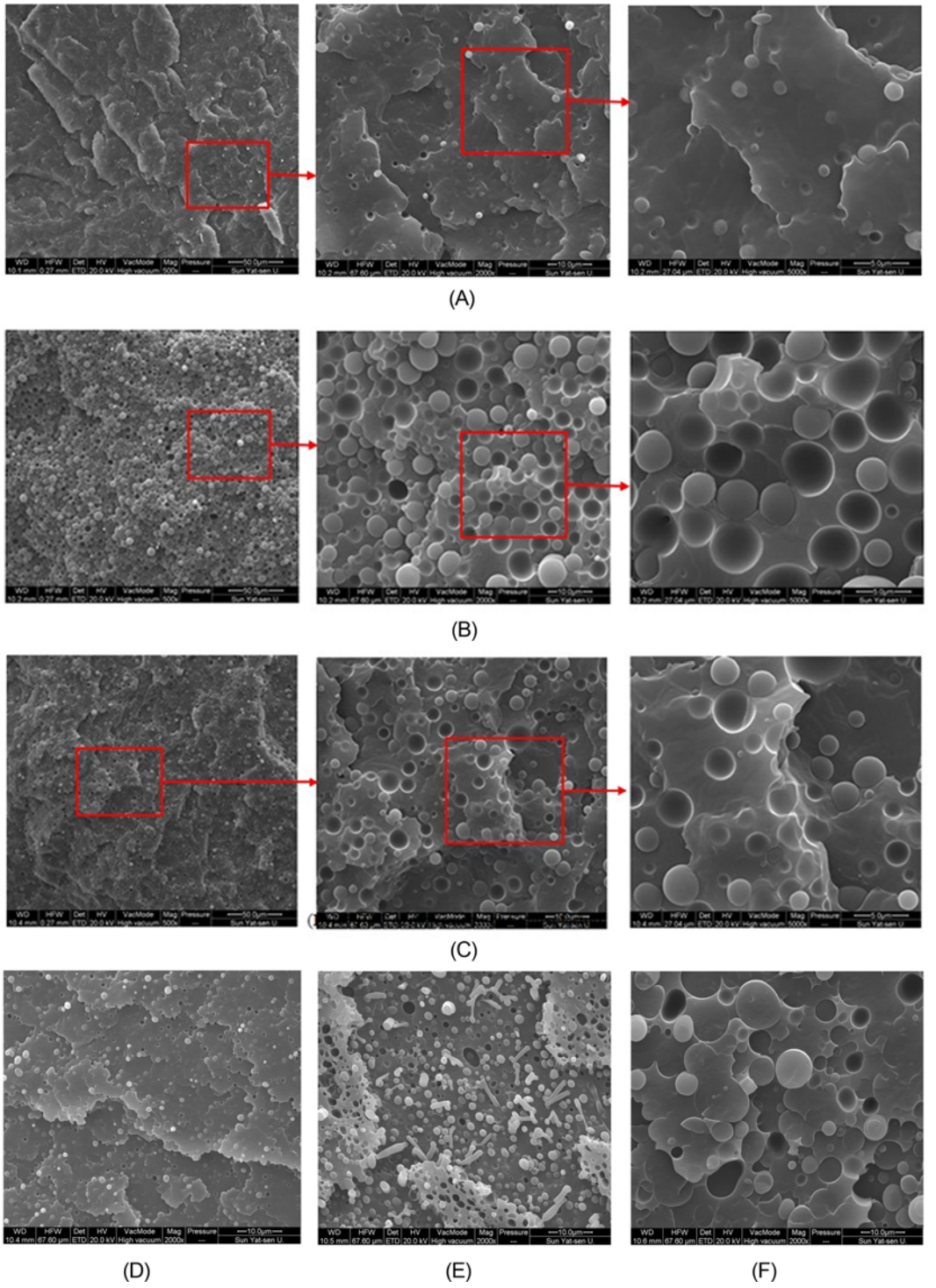

Figure 6. Phase morphology of NTSE-extruded TPU/PP blends; (A) 10 % TPU of different amplification factors, (B) 70 % TPU of different amplification factors, (C) 90 % TPU of different amplification factors, (D) 20 % TPU, (E) 30 % TPU, and (F) 50 % TPU.

increased with increasing TPU content (⩽50 %). These changes are perhaps attributed to the coalescence of several small particles with increasing TPU content. Interestingly, for the cases of NTSE-extruded blend with 30 % TPU content and TSE-extruded blend with 50 % TPU content, the dispersed phase (TPU) shows some fibrous elements. For other cases, the shape is spherical.

The fractured surface of the blend prepared with TSE was

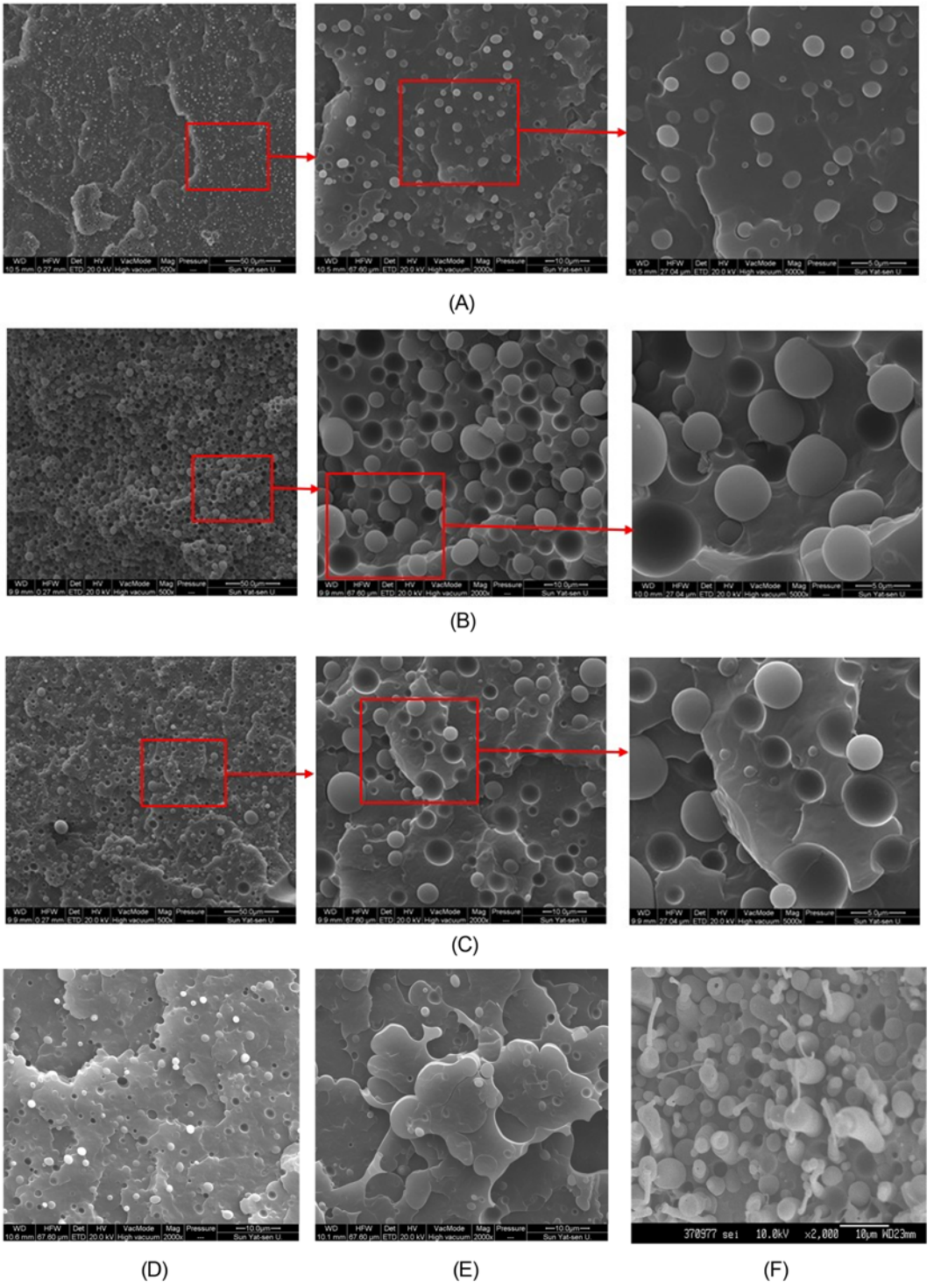

Figure 7. Phase morphology of TSE-extruded TPU/PP blends; (A) 10 % TPU of different amplification factors, (B) 70 % TPU of different amplification factors, (C) 90 % TPU of different amplification factors, (D) 20 % TPU, (E) 30 % TPU, and (F) 50 % TPU.

more smooth with a number of similarly parallel cracks and presented typical fragility performance (Figure 7(A)), in contrast, the fractured surface of the blend prepared with NTSE was somewhat multilayer structure with the cracks having different orientations (Figure 6A). It follows that the impact strength of the blend extruded by NTSE was higher than that of the blend prepared with TSE. The particle size of dispersed phase of NTSE-extruded blend with 70 % TPU

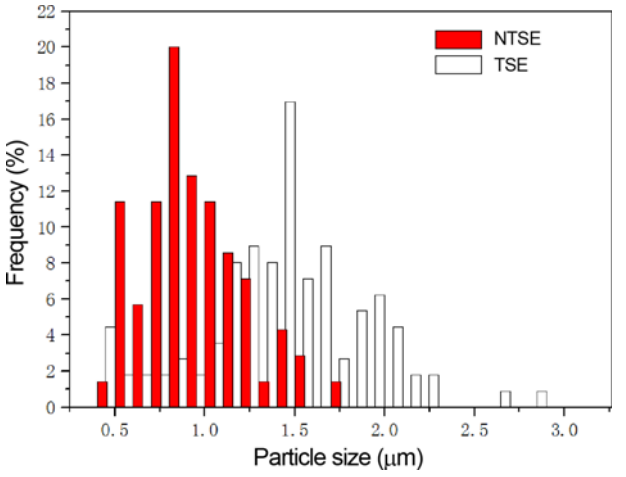

Figure 8. Distribution of dispersed particles of blends with 10 % TPU weight content.

content (Figure 6(B)) is smaller than that of dispersed phase of TSE-extruded blend with 70 % TPU content (Figure 7(B)), which agreed with the mechanical properties discussed above. Some extremely large particles were found in TSE-extruded blend with 90 % TPU content (Figure 7(C)). The NTSE-extruded blend with 90 % TPU content (Figure 6(C)) had rougher fractured surface and the particle size of dispersed phase is smaller compared to those of TSE-extruded blend (Figure 7(C)). More importantly, dispersed TPU forms long fibers with a large aspect ratio from the Figure 6(E) observation. The interface between the TPU and PP matrices is sharp because of high interfacial tension. The formation of TPU particles is clearly observed. This phenomenon is attributed to the fact that some fibers are broken up and particles are changed under the influence of the reinforcement of the flow field in NTSE. And the compatibility between PP and TPU was improved when NTSE was used.

Table 4. Average diameter (μm) of particles in blends prepared by non-twin screws extruder and twin-screw extruder

Blends	TPU/PP					
Content ration	10/90	20/80	30/70	50/50	70/30	90/10
Non-twin screw extruder	0.89	0.72	1.09	2.51	2.84	1.97
Twin-screw extruder	1.48	1.30	1.46	2.93	4.15	3.12

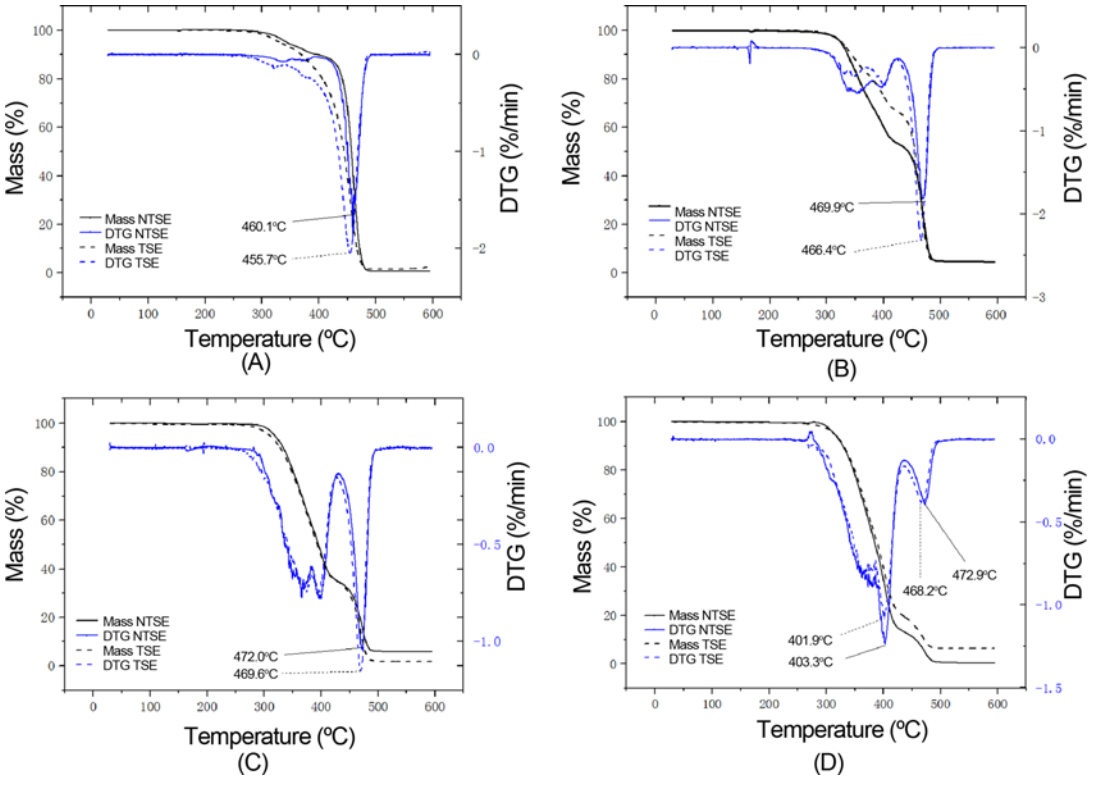

Figure 9. Thermal decomposition behavior of the blends extruded by NTSE and TSE; (A) 10 % TPU, (B) 50 % TPU, (C) 70 % TPU, and (D) 90 % TPU.

Figure 8 shows the distribution of dispersed particles of blends with 10 % TPU weight content prepared with NTSE and TSE. The diameters of dispersed particles of NTSE-extruded blend ranged from 0.39 μm to 1.66 μm and the average diameter was 0.89 μm. While the diameters of dispersed particles of TSE-extruded blend ranged from 0.48 μm to 2.92 μm and the average diameter was 1.48 μm. The average diameter decreased, and the distribution narrowed for blend with 10 % TPU content extruded by NTSE compared to those of TSE-extruded blend with 10 % TPU content. The dissimilarity proves that the mechanical properties of NTSE-extruded specimens are better than those of TSE-extruded samples and NTSE has higher dispersive mixing efficiency than TSE.

Table 4 shows the average diameter of dispersed phase for TPU/PP blends with different content ratio. The diameters of dispersed phase in blends prepared with NTSE and TSE ranged from 0.72 to 2.84 μm and 1.30 to 4.15 μm, respectively. The average diameters of dispersed phase for NTSE-extruded blends were smaller than those of TSE-extruded blends with high TPU content, which was consistent with the mechanical properties results. The data shows clearly that the particle size of dispersed phase in TPU/PP blends prepared with the former processing method was smaller than that prepared with the latter.

Thermostability Properties Analysis

Thermogravimetric analysis (TGA) and corresponding differential thermogravimetric analysis (DTG) results for various TPU/PP blends extruded by NTSE and TSE are shown in Figure 9. The minimum peak temperature of degradation for NTSE-extruded blends influenced by the flow field was about 1 and 4 °C higher than for those extruded by TSE, respectively. The temperature (T_1) of the DTG curves shows the temperature at which the initial weight loss was performed and T_3 represents the terminal degradation temperature, as shown in Table 5. T_1 of the specimens extruded by NTSE was delayed by about 14, 3 and 6 °C as compared to T_1 for those extruded by TSE. T3 of the specimens extruded by NTSE was delayed by about 3, 3, 2, and 3 °C as compared to T_3 for those extruded by TSE. These results suggest that the effect of the flow field on the thermal stabilities of NTSE-extruded TPU/PP blends was very evident and the interaction of them was stronger.

Table 5. TG parameters of the TPU/PP blends extruded by NTSE and TSE

Content	Extruder	T_1	T_3
10 wt % TPU	NTSE	306.92	472.10
	TSE	292.47	469.32
50 wt % TPU	NTSE	317.64	478.87
	TSE	315.07	476.25
70 wt % TPU	NTSE	319.39	482.31
	TSE	312.91	480.48
90 wt % TPU	NTSE	317.92	483.18
	TSE	317.60	480.35

Conclusion

We investigated the mechanical properties, morphology properties and thermal stabilities of the TPU/PP blends extruded by the novel self-made co-rotating non-twin screws extruder and the traditional co-rotating twin-screw extruder, respectively. Here two types of extruders had the same diameters and centerline distances. The screw with two tips was set at the same speed for both extruders and nearly equal outputs was chosen. Although the novel NTSE had only two thirds screw length of the traditional TSE and had fewer kneading disks, the mechanical properties (i.e., tensile strength, elongation at break, tensile modulus, and impact strength) of TPU/PP blends extruded by NTSE were still superior to those prepared with the traditional TSE. The processing method for NTSE reduced the particle size of dispersed phase and narrowed the distribution at the same time, compared to the traditional TSE method. According to the TG curves of the TPU/PP blends, the thermal stabilities of the TPU/PP blends extruded by NTSE were better than those of blends prepared with TSE. These results indicate that the mixing performance influence by the reinforcement of flow field in novel NTSE was superior to shear flow in traditional TSE.

Acknowledgement

The present study was supported by the National Natural Science Foundation of China (No. 11272093) for which the authors are grateful. Project was also supported by Guangdong Province Higher Vocational Colleges & Schools Pearl River Scholar Funded Scheme (2012) and State Scholar Fund of China (2013).

References

1. J. Varga, *J. Mater. Sci.*, **27**, 2557 (1992).
2. S. H. Ajili, N. G. Ebrahimi, and M. T. Khorasani, *J. Appl. Polym. Sci.*, **89**, 2496 (2003).
3. M. Szycher, "Szycher's Handbook of Polyurethanes", CRC Press, New York, 1999.
4. C. W. Macosko and Q. W. Lu, *Polymer,* **45**, 1981 (2004).
5. P. Potschke, K. Wallheinke, H. Fritsche, and H. Stutz, *J. Appl. Polym. Sci.*, **64**, 749 (1997).
6. P. Potschke, J. Pionteck, and H. Stuz, *Polymer*, **43**, 6965 (2002).
7. M. Kannan, S. S. Bhagawan, K. Joseph, and S. Thomas, *Polymer Plast. Tech. Eng.*, **48**, 871 (2009).
8. P. Potschke and K. Wallheinke, *Polym. Eng. Sci.*, **39**, 1035

(1999).
9. J. P. Qu, G. J. He, and H. Z. He, *J. Eur. Polym.*, **40**, 1849 (2004).
10. H. P. Grace, *Chem. Eng. Commun.*, **14**, 225 (1982).
11. L. A. Utracki and Z. H. Shi, *Polym. Eng. Sci.,* **32**, 1824 (1992).
12. J. M. H. Janssen and H. E. H. Meijer, *J. Rheol.*, **37**, 597 (1993).
13. C. E. Scott and C. W. Macosko, *Polymer,* **36**, 461 (1995).
14. J. Kong, T. G. Simth, and D. I. Bigio, *J. AIChE*, **42**, 649 (1996).
15. Y. Suzaka, *U.S. Patent*, 4,334,783 (1982).
16. X. Q. Nguyen, D. Ormeaux, and L. A. Utracki, *U.S. Patent*, 5,4511,06A (1995).
17. J. P. Qu, *CN Patent*, 200810026054.X (2008).
18. B. P. Xu, *CN Patent*, 201010201316.9 (2010).
19. B. P. Xu and H. W. Yu, *J. Adv. Mater. Res.*, **560-561**, 1091 (2012).
20. M. L. Booy, *J. Appl. Polym. Sci*., **18**, 973 (1978).
21. C. Hepburn, "Polyurethane Elastomers", Applied Science, London, 1982.
22. X. Zhang and Z. Yin, *J. Appl. Polym. Sci.,* **62**, 893 (1996).
23. S. K. Jia, J. P. Qu, W. F. Liu, C. R. Wu, R. Y. Chen, S. F. Zhai, and Z. Huang, *Polym. Eng. Sci.,* DOI:10.1002/pen. 23598 (2013).